

Study of Noise Analysis of Front-End Readout Systems in Hadronic Calorimeter at CMS Experiment at Large Hadron Collider

Kadri ÖZDEMİR^{1*}

¹ Izmir Bakircay University, Faculty of Engineering and Architecture Faculty, Department of Fundamental Sciences, Izmir, Turkey

kadri.ozdemir@bakircay.edu.tr, ORCID: 0000-0002-0103-1488

Abstract: The Hadronic Calorimeter (HCAL) in the CMS experiment at the Large Hadron Collider (LHC) at CERN has been designed to measure the energy of jets which are the signature of quark and gluons produced in strong interactions. The jet measurements is the crucial importance for both detector performance and studies Standard Model (SM) and Beyond the Standard Model (BSM) physics analyses such as supersymmetry (SUSY), Higgs boson and heavy gauge boson researches. The other important feature of jet measurements is that it tests the performance of simulated proton-proton (pp) collision data produced with Monte Carlo (MC) simulations. Precise and accurate measurement of jets of great importance in HCAL especially in central region of the calorimeter ($|\eta| < 3.0$) and concerns many physics analyzes performed in the CMS experiment. Very large aberrant GeV-TeV scale noise is detected in the Hadronic Barrel (HB) and Hadronic Endcap (HE) sub-detectors located in the central area of HCAL, and it was understood that these GeV-TeV scale noise is not caused by pedestal and other noises. The GeV-TeV scale noise is due to the Front-End Readout Systems in the HB and HE calorimeters. The characteristics and analysis of the noise originating from the GeV-TeV scale Front-End Readout Systems in the HB and HE calorimeters are presented in this study for both 0 T and 3.8 T magnetic field.

Keywords: CMS , Hadronic Barrel, Hadronic Endcap, Noise, Readout Systems

Büyük Hadron Çarpıştırıcısındaki CMS Deneyinde Hadronik Kalorimetrenin Ön-Uç Okuma Sistemlerinin Gürültü Analizinin İncelenmesi

Özet: CERN'deki Büyük Hadron Çarpıştırıcısındaki (BHÇ) CMS deneyinde bulunan Hadronik kalorimetre (HKAL), güçlü etkileşimlerde üretilen kuark ve gluonların imzası olan jetlerin enerjisini ölçmek için tasarlanmıştır. Jetlerin ölçümleri, hem dedektör performansı hem de Süpersimetri (SUSI), Higgs bozonu ve ağır ayar bozon araştırmaları gibi Standart Model (SM) ve Standart Model Ötesi (BSM) fizik analiz çalışmaları için büyük önem taşımaktadır. Jet ölçümlerinin bir diğer önemli özelliği ise Monte Carlo (MC) simülasyonları ile üretilen benzetilmiş proton-proton (pp) çarpışma verilerinin performansını test etmesidir. HCAL'de özellikle kalorimetrenin merkez bölgesindeki ($|\eta| < 3.0$) jetlerin hassas ve doğru ölçümü CMS deneyinde gerçekleştirilen birçok fizik analizini ilgilendirmektedir. HCAL'in merkezi bölgesinde bulunan Hadronik Fıçısı (HB) ve Hadronik Uç-kapak (HE) alt detektörlerinde çok büyük anormal GeV-TeV mertebesinde gürültü saptanmış olup, bu GeV-TeV mertebesinde gürültünün pedestal ve diğer gürültülerden kaynaklanmadığı anlaşılmıştır. GeV-TeV mertebesindeki gürültünün nedeni HB ve HE kalorimetrelerindeki ön-uç readout sistemlerinden kaynaklanmaktadır. Bu çalışmada, HB ve HE kalorimetrelerindeki GeV-TeV ölçeğindeki ön-uç readout sistemlerinden kaynaklanan gürültünün özellikleri ve analizi 0 T ve 3.8 T'lik manyetik alan için sunulmaktadır.

Anahtar Kelimeler: CMS , Hadronik Fıçısı, Hadronik Uç-Kapak, Gürültü, Readout Sistemleri

Reference to this paper should be made as follows (bu makaleye aşağıdaki şekilde atıfta bulunulmalı):
Kadri Özdemir, 'Study of Noise Analysis of Front-End Readout Systems in Hadronic Calorimeter at CMS Experiment at Large Hadron Collider', Elec Lett Sci Eng, vol. 19(1), (2023), 8-16.

* Corresponding author; kadri.ozdemir@bakircay.edu.tr

1. INTRODUCTION

The LHC [1] is installed in the LEP tunnel at CERN to conduct high-energy physics research. The LHC is a 26.7 km long a ring of superconducting magnets with a series of accelerator structures, that is the world's most powerful and largest accelerator. Although the LHC is designed to collide proton beams with a center-of-mass energy of 14 TeV, it plans to reach this targeted energy in the LHC Run-III phase, which has just begun. In the LHC Run-I phase, proton beams were operated at center-of-mass energies of 7 and 8 TeV between 2009 and 2013, the Higgs boson [2,3] with a mass of 125 GeV was discovered during this phase. LHC Run-II was operated at center-of-mass energies of 13 TeV proton-proton (pp) collision between 2015 and 2018 which leads to observation of rare Vector Boson Scattering process and 4-top-quarks.

The ATLAS [4], CMS, ALICE [5] and LHCb [6] detectors are located at four locations in the LHC where proton beams are collide. The ATLAS and CMS experiments are general purpose detectors for investigating all aspects of SM and BSM physics. The LHCb detector is designed to probe b-physics, while the ALICE detector is designed to probe heavy ion physics.

CMS [7] is a general purpose detector designed to discover Higgs boson and new heavy vector bosons, to search for SUSY particles, Exotic particles and extra dimensions and to study QCD, flavor and electroweak physics. Therefore, the CMS detector is designed in a hermitic structure and consists of sub-detectors from the inside out. The tracker system [8] is located in the innermost part of the CMS detector and is designed to measure the trajectory of charged particles and reconstruct the secondary vertices with precision. The CMS detector has an a lead tungstate crystal Electromagnetic Calorimeter (ECAL) [9] after the tracker, and is designed to detect electrons and photons and measure their energies. The HCAL, which is the main subject of this study, surrounds the ECAL and is designed to precisely measure jets and missing transverse energy (mostly neutrinos or exotic particles). The solenoid magnet is placed between HCAL and the muon systems which provides a magnetic field of 3.8 T. The both hadronic outer calorimeter that is designed to measure lately started hadronic showers or in the other word high energetic jets, and muon spectrometer [10] are placed outside of the solenoid.

The precise measurements of hadronic jet has not only the the key importance the CMS physics goal but also detector performance and test the performance of simulated pp collision data produced with MC simulations. In order to measure jets in calorimeter precisely, the characteristic of the noise of the calorimeter should be thoroughly understand and suppress from the calorimeter signal. In this reason, next section is devoted to HCAL detector structures and front-end readout systems especially HB and HE. The anomalous GeV-TeV scale noise is due to the front- end readout systems in the HB and HE calorimeters and both characteristics and analysis of this noise will be discussed in the Results and Discussion section.

2. MATERIAL AND METHODS

In general, the energy of particle is measured in calorimeters. More specifically, when the particle enters the calorimeter, it initiate particle showers, and then the energy of particles coming from the shower is deposited in the calorimeter and finally the deposited energy of the particles coming from the shower is measured in the calorimeter. Calorimeter consist of ECAL and HCAL in the CMS detector. The length of the active material of the calorimeter is determined by the radiation length for ECAL and the nuclear interaction length for HCAL. In this section, detailed HCAL detector structures and front-end readout systems will be discussed.

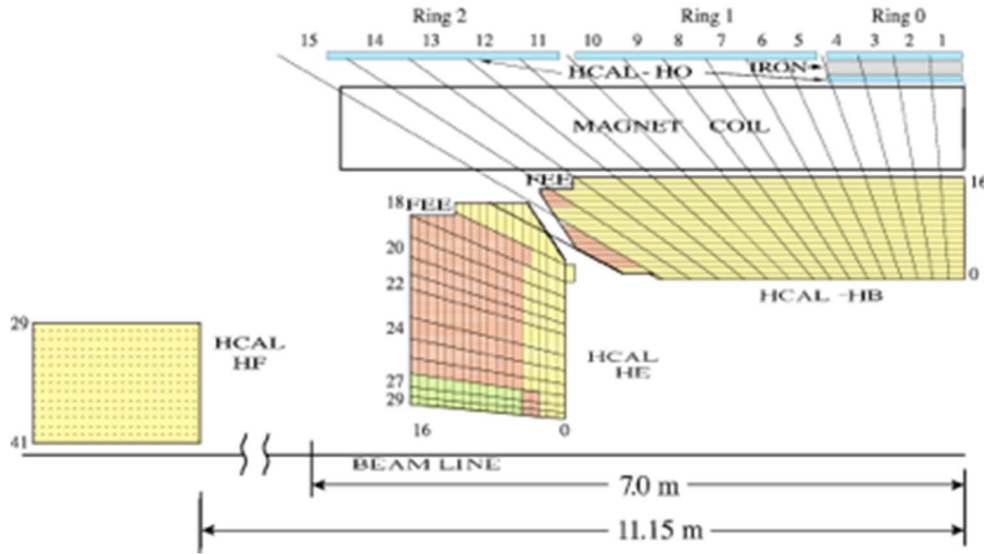


Figure 1. Quarter view of HCAL[11].

HCAL [11] is a sampling calorimeter, plastic scintillator is used as active material, flat iron and steel layers are used as passive material absorber. HCAL consists of four sub-detectors: HB, HE, Hadron Outer (HO) and Hadron Forward (HF). The quarter view of the HCAL is shown in Figure 1. The HB [12] rapidity ranges up to $|\eta| < 1.3$ and is splitted into two half-barrel sections called HB+ and HB-. HB has a 36 identical wedge with 20° and it is form of flat brass/steel absorber its sampling structure [12]. Each flat brass/steel absorber sliced into four sector in the ϕ direction which means 5° for each sector. Plastic scintillator tiles placed between stainless steel and brass absorber plates form the active element of the sampling HB calorimeter. It is divided into 32 sectors in total, each sector is called “tower” in HCAL. Each half-barrel of HB has 16 η towers. 15^{th} - 16^{th} η towers sliced in depth because of the read out boxes placement causing space constraint. In the CMS experiment, as in all experiments at the LHC, the energy and momentum of the particles are measured in terms of pseudorapidity (η) and azimuth angle (ϕ), but index eta ($i\eta$) and index phi ($i\phi$) values are used in HB and HE calorimeters which is indicate the projective tower or define the each HB and HE tower. The $i\eta$ and $i\phi$ values or definition is also used for HB and HE front-end readout systems that makes easier mapping of HB and HE channels in read out sytems. HE covers $1.3 < |\eta| < 3.0$ rapidity region which has different and more complex geometry than HB, has same number of tower with HB. Since both HB and HE have same number of tower, their front-end readout systems are exactly same. HO [13] covers $|\eta| < 1.26$ which is designed to measure initiating lately showering particles before the muon system, therefore its geometry was chosen respect to muon system different from the HB and HE geometry. HF [14] covers $1.3 < |\eta| < 3.0$ rapidity region that is located very close to beam pipe. The main difference of HF than HB and HE is front-end readout system using Photo Multiplier Tubes (PMTs).

Since this study is based on HB and HE readout systems, only the front-end readout systems of these two detectors will be described here. The front-end readout system of HB and HE consists of hybrid photodiode (HPD), charge-integrator and encoder (QIE) card, channel control ASIC (CCA) and Gigabit Optical Link (GOL) and are called readout boxes (RBX). The HB and HE optical system is directly related to the RBXs of these detectors (See Figure 2). The particles passing through the plastic scintillator tiles in the HB and HE detectors emit a light in direct proportion to their own energy. The the wavelength-shifting (WLS) fibers in the figure 2 are embedded in plastic scintillator tiles and collect the emitted light and transmit it to the HPDs with the help of waveguides and optical cables.

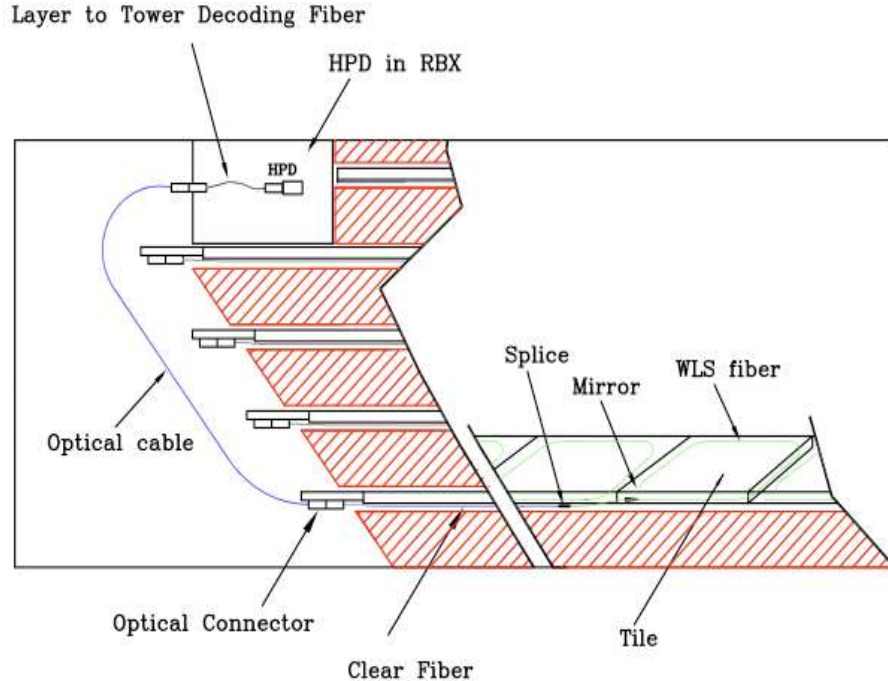


Figure 2. Schematic of the HB systems [7].

Light transmitted via optical cables is connected to the optical-decoding unit (ODU) with each tower mapped to correspond to individual pixels on HPDs. Simply HPDs convert optical signal to electrical signal. The signal from the HPD is converted into the digital signal by the QIE, which contains four capacitors converting the charge by a 7-bit analogue-to-digital converter (ADC) every 25 ns. CCA supply clocks to the QIEs. It also synchronizes and monitors data from multiple QIEs and finally this digital signal output feeds into the GOL at 40 Hz. HB and HE RBX and HPD, QIE, CCA and GOL inside it is shown in Figure 3.

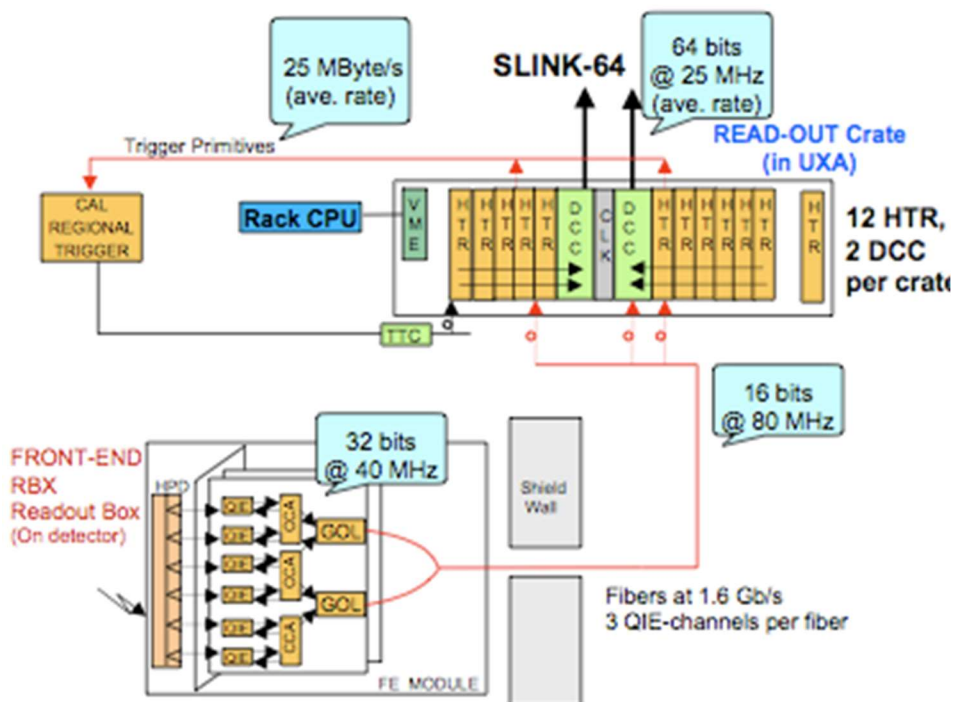


Figure 3. Overview of HB and HE RBX and readout systems [15].

3. RESULTS AND DISCUSSION

Very large aberrant GeV-TeV scale noise is observed in the HB and HE detectors and it was understood that these GeV-TeV scale noise is not caused by pedestal and other noises. The noise is due to the RBXs in the HB and HE. The characteristics and analysis of the noise originating from the GeV-TeV scale RBXs in the HB and HE calorimeters are investigated in this study for both 0 T and 3.8 T magnetic field. The purpose of this analysis is to detect noisy RBXs or HPDS in the HB and HE.

HB has 32 wedges which means 32 RBXs for each half-barrel sections. Both HB+ and HB- has 16 RBXs. Each RBXs has 4 HPDs (See Figure-4) also called Readout modules (RMs) as well which is represent successive ϕ direction with 5° . Totally HB has 144 HPDs, 72 each for the HB+ and HB-. Each HPD has 18 channels corresponding to 16 sequential towers including the last two with two depths [16]. Figure 4 shows the illustration the HB RBX channel mapping. As mentioned before, HB and HE has the same RBX channel mapping.

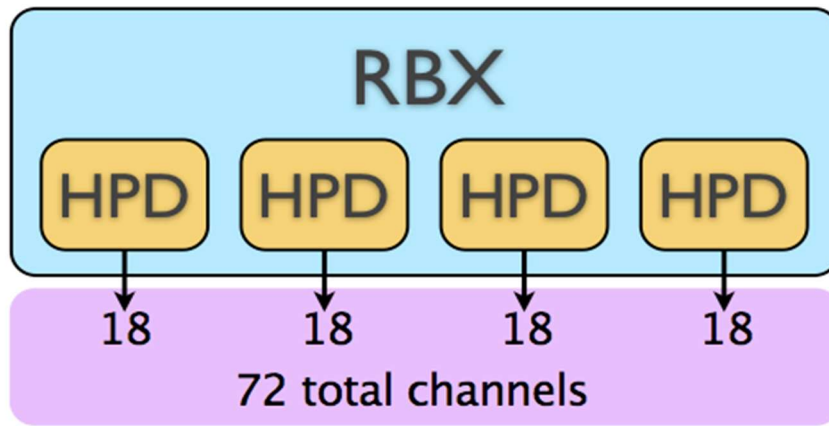


Figure 4. Illustration of the HB RBX channel mapping [17].

In HB and HE it is not possible to measure the jet energy signal in a single time slices (TS) of 25 ns, so this signal is reconstructed using 10 time intervals. During Global and Local data taking, the energy and time of signal are reconstructed by using 4 consecutive TS instead of 10 TS for both HB and HE. The unit of charge used in this study is the femto Coulomb (fC), and 1fC in HB and HE corresponds to approximately 0.2 GeV and 0.3 GeV respectively. The HBHE self-trigger local runs are used in this analysis which were taken since 2010 at 0 T and 3.8 T magnetic field. Totally 152 HBHE self-trigger local runs are analyzed and each HBHE self-trigger local run has 5000 events.

The CMSSW_6_2_1 version of the CMS software based on the C++ programming language is used. ROOT software framework is used as well. When self-trigger local runs are examined, a large number of ADC=0 values are detected and the reason for this behavior is not understood well, but it is concluded that the large number of ADC=0 values it associated with HPDs/RRXs noise. The number of ADC=0 values are chosen as first criteria to characterize the GeV-TeV noise.

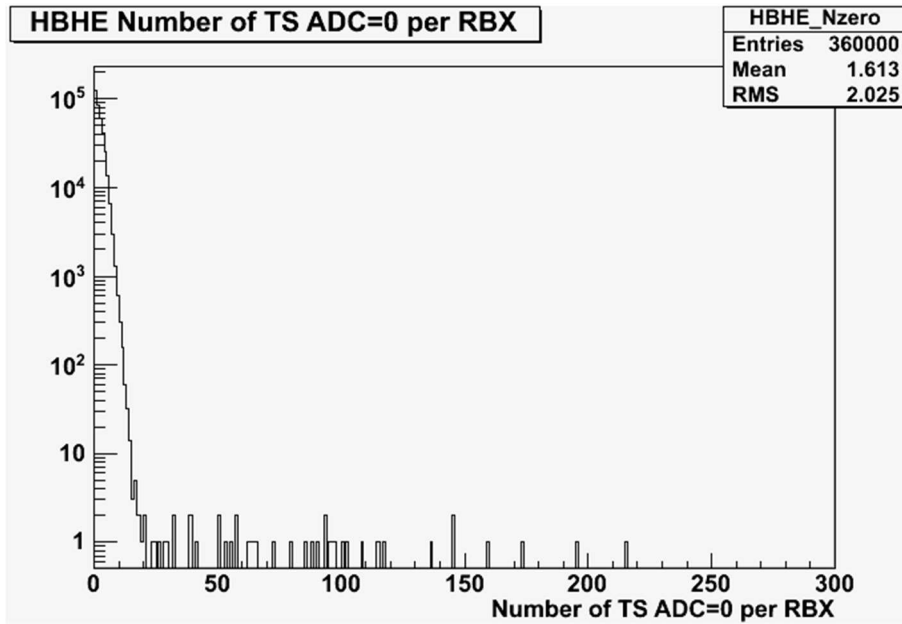


Figure 6. The number of ADC=0 in 4 TS of all channels per RBXs for both HB and HE for self-trigger local run 140575

Figure 5 shows for self-trigger local run 140575 the number of ADC=0 in 4 TS of all channels per RBXs for both HB and HE. When the figure 5 is examined, it is easily understood that the number of ADC=0 bigger than 20 should be excluded from this analysis because of not enough statistics. The number of ADC=0 < 20 value is chosen as first criteria or cut to characterize the GeV-TeV noise. In order to be sure about this cut, the noise rates versus RM index are plotted for the number of ADC=0 < 20 (Figure 6 upper) and ADC=0 > 20 (Figure 6 lower) selection criteria which good reference run (127777) are compared to run 130289. As seen Figure 6, ADC=0 > 20 value is excluded from analysis because of low statistic and very low noise rates.

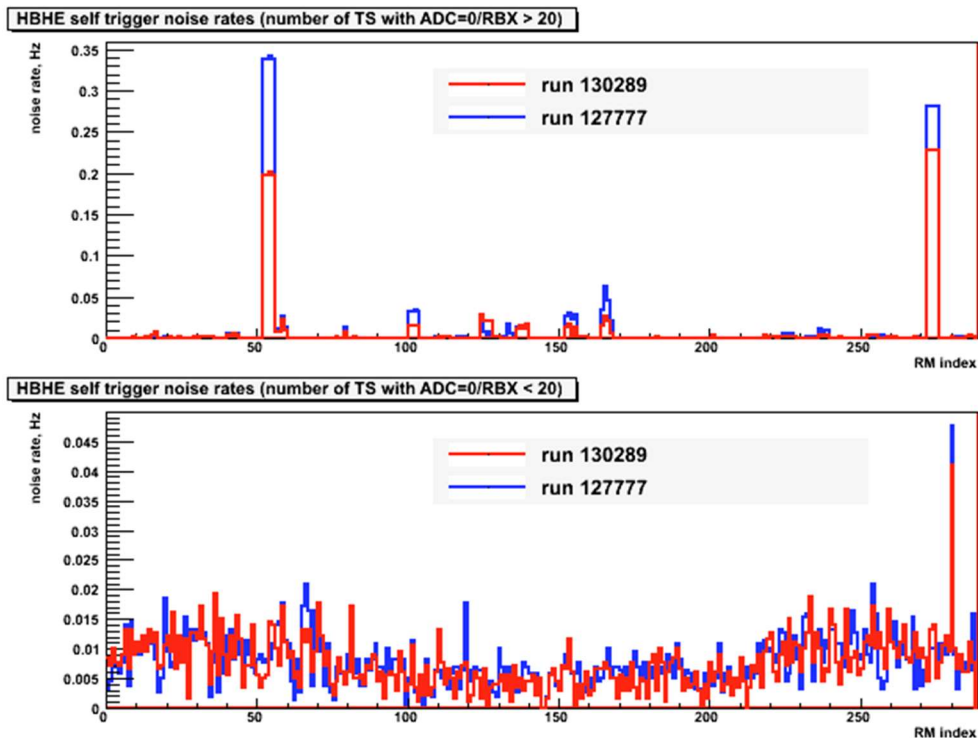


Figure 7. The noise rates versus RM index for the number of ADC=0 < 20 (upper) and the ADC=0 > 20 (lower) for 127777 (good reference run) and 130289.

The energy of the pixels, $E > 3$ GeV, cuts are applied as second criteria in order to subtract to pedestal noise from the analysis. Then the pixel multiplicity with $E > 3$ GeV are plotted to characterize the noise in the HB and HE for run 143530. As seen in Figure 8, the three distinctive peak of the pixel multiplicity with $E > 3$ GeV in the is observed and categorized.

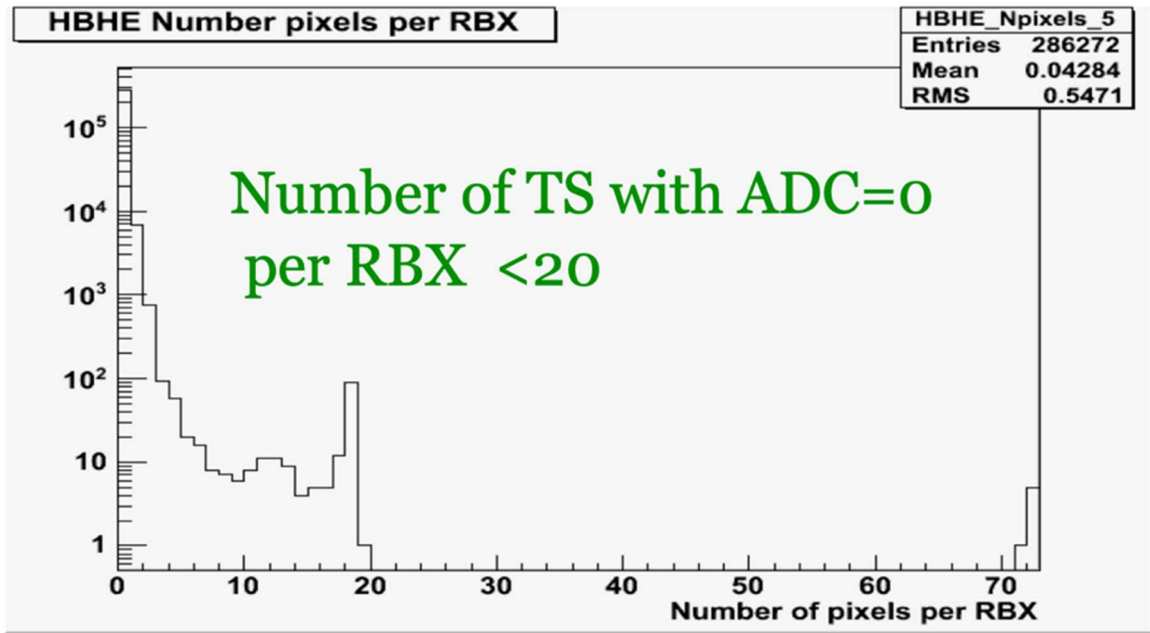


Figure 8. The pixel multiplicity with $E > 3$ GeV for run 143530.

First peak of the pixel multiplicity with $E > 3$ GeV is observed between 1-10 and defined as HPD ion feedback [17], generating considerable signals because of a thermally emitted electron ionizing a gas or by surface molecule. Second peak of the pixel multiplicity with $E > 3$ GeV is observed between 11-25 and defined as HPD discharge [17] because of an electrical discharge spreading from HPD's wall. Second peak of the pixel multiplicity with $E > 3$ GeV is observed between 26-72 and defined as RBXs noise which has no possibility to all HPDs noisy because of ion feedback or discharge. The noise is investigated under two selection criteria with three conditions separately and no noisy HPDs found because of HPD discharge and RBX noise from the 152 HBHE self-trigger local runs.

HPD ion feedback conditions are investigated carefully and the noise rates are plotted as seen Figure 9. The noise rates for HPD ion feedback is obtained as 0.08 Hz. Then each RBX HPDs noise rates plotted as a function of 30 runs roughly as seen in Figure 10. The noisy HPDs of each RBXs are determined and listed. RBX No 02 HPD No 03, RBX No 07 HPD No 02, RBX No 08 HPD No 02 and RBX No 1 HPD No 04 are the noisy HPDs of the HB- in total. In HE calorimeter has only one noisy HPDs and it is RBX No 16 HPD 03 of the HE+.

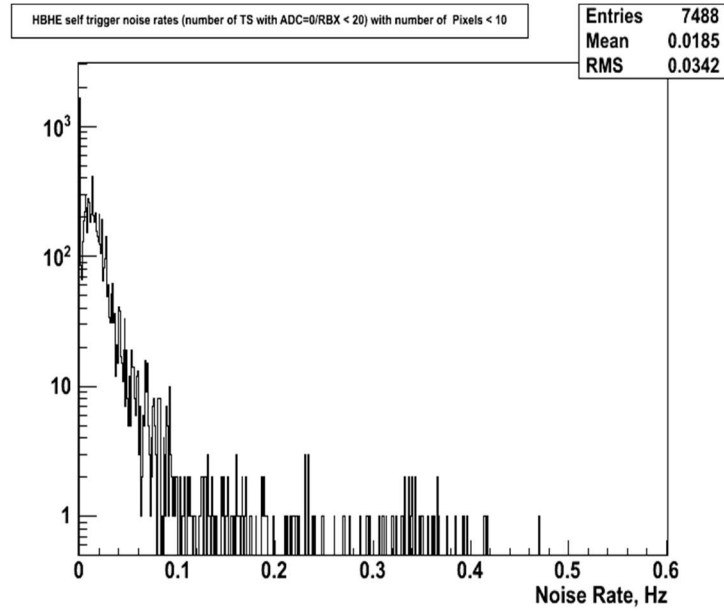


Figure 9. The noise rates of HPD ion feedback for run 143530.

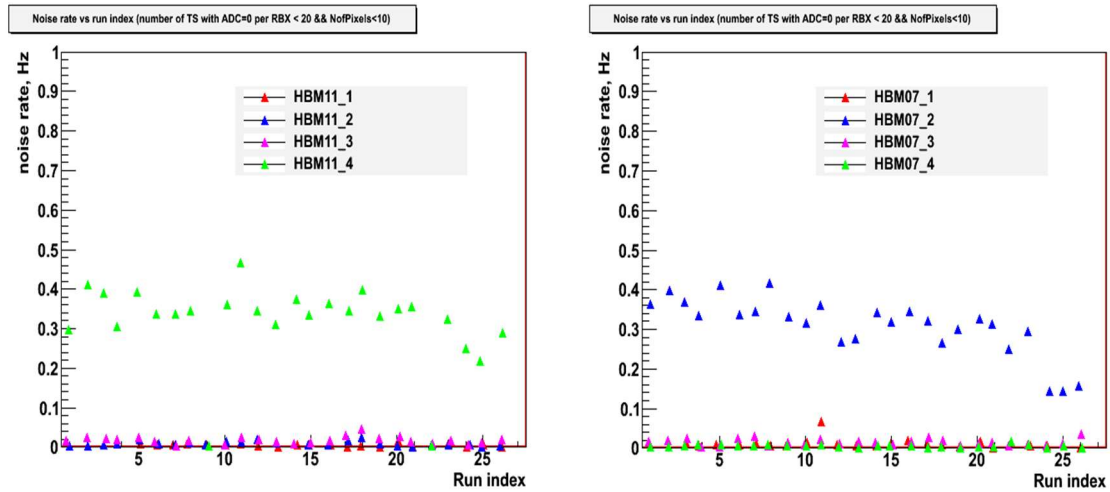


Figure 10. RBX No 11 and RBX No 07 HPDs noise rates plotted as a function of 30 runs roughly for run 143530.

4. CONCLUSIONS

Very large aberrant GeV-TeV scale noise is observed in the HB and HE detectors and it was understood that these GeV-TeV scale noise is not caused by pedestal and other noises. The noise is due to the RBXs in the HB and HE. This noise is characterized as HPD ion feedback, HPD discharge and RBX noises after this study. No noisy HPDs are identified as HPD discharge and RBX noise from the 152 HBHE self-trigger local runs. RBX No 02 HPD No 03, RBX No 07 HPD No 02, RBX No 08 HPD No 02, RBX No 1 HPD No 04 are the noisy HPDs of the HB- due to ion feed back and also in HE+ of RBX No 16 HPD 03. The signal of those noisy HPDs were suppressed to precise and accurate measurement of jets after this study. Then, the noisy HPDs were replaced with new ones.

References

- [1] L. R. Evans and P. Bryant, "LHC Machine", JINST, 3 (2008) S08001, 2008.
- [2] S. Chatrchyan et al. (CMS), "Observation of a new boson at a mass of 125 GeV with the CMS experiment at the LHC", Physics Letters B, 716 (2012) 30, 2012.
- [3] G. Aad et al. (ATLAS Collaboration), "Observation of a new particle in the search for the Standard Model Higgs boson with the ATLAS detector at the LHC", Physics Letters B, 716 (2012) 1-29, 2012.
- [4] G. Aad et al. (ATLAS Collaboration), "ATLAS Experiment at the CERN Large Hadron Collider", Journal Of Instrumentation, 3 (2008) S08003, 2008.
- [5] K. Aamodt et al. (ALICE Collaboration), "ALICE Experiment at the CERN Large Hadron Collider", Journal Of Instrumentation, 3 (2008) S08002, 2008.
- [6] A. A. Alves et al. (LHCb Collaboration), "LHCb Detector at the CERN Large Hadron Collider", Journal Of Instrumentation, 3 (2008) S08005, 2008.
- [7] S. Chatrchyan et al. (CMS Collaboration), "CMS Experiment at the CERN Large Hadron Collider", Journal Of Instrumentation, 3 (2008) S08004, 2008.
- [8] V. Khachatryan et al. (CMS Collaboration), "Description and performance of track and primary-vertex reconstruction with the CMS tracker", Journal Of Instrumentation, 9 (2014) P10009, 2014.
- [9] V. Khachatryan et al. (CMS Collaboration), "Performance and operation of the CMS electromagnetic calorimeter", Journal Of Instrumentation, 5 (2010) T03010, 2010.
- [10] S. Chatrchyan et al. (CMS Collaboration), "Alignment of the CMS muon system with cosmic-ray and beam-halo muons", Journal Of Instrumentation, 3 (2010) T03020, 2010.
- [11] S. Chatrchyan et al. (CMS Collaboration), "Performance of the CMS Hadron Calorimeter with Cosmic Ray Muons and LHC Beam Data", Journal Of Instrumentation, 5 (2010) T03012, 2010.
- [12] S. Abdullin et al., "Design, performance, and calibration of the CMS hadron-barrel calorimeter wedges," European Physical Journal C, 55, 1 (2008) 159-171, 2008.
- [13] S. Abdullin et al., "Design, performance, and calibration of the CMS hadron-outer calorimeter," European Physical Journal C, 57, 3 (2008) 653-663, 2008.
- [14] G. Baitaian et al., "Design, Performance, and calibration of the CMS Forward Calorimeter Wedge," European Physical Journal C, 53 (2008) 139-166, 2008.
- [15] G. Baitaian et al., "CMS Physics Technical Design Report, Volume I: Detector Performance and Software", CMS TDR 8.1, 2006.
- [16] Chou P. J. et al., "Anomalous HB/HE Noise Startup: Characteristics and Rejection Algorithms", CMS IN-2010/006., 2010.
- [17] S. Chatrchyan et al. (CMS Collaboration), "Identification and Filtering of Uncharacteristic Noise in the CMS Hadron Calorimeter", Journal Of Instrumentation, 5 (2010) T 03014, 2010.